ANION PHOTOELECTRON SPECTROSCOPY AND HIGH LEVEL AB INITIO CALCULATIONS OF THE HALIDE-ACETYLENE DIMER COMPLEXES

D. A. R. Beckham S. Conran K. M. Lapere M. Kettner
A. J. McKinley D. A. Wild*

School of Chemistry and Biochemistry
The University of Western Australia
M310, 35 Stirling Hwy, Crawley, Australia 6009
duncan.wild@uwa.edu.au

ABSTRACT: Anion photoelectron spectra are presented for the halide-acetylene complexes, $X^- \cdots C_2H_2$ where X = Cl, Br, and I. Electron binding energies are determined to be 4.1, 3.8 and 3.4 eV respectively. Results from CCSD(T) calculations are presented for the neutral halogen-acetylene complexes. Two minima are predicted corresponding to a linear $C_{\infty v}$ and T-shaped C_{2v} geometry, with the T-shaped geometry stationary point predicted to be the global minimum. The form of the photoelectron spectrum is determined via prediction of the Franck-Condon factors linking the anion and neutral states.

*Author to whom correspondence should be addressed.

1 Introduction

Anion photoelectron spectroscopy of gas phase complexes is an invaluable tool for characterising intermolecular interactions. The major piece of information derived from the experiment is the electron binding energy of the neutral complex, however one can also map out the neutral potential energy surface should the spectrum display vibrational resolution. The information gleaned from the spectra is of importance in predicting reaction directions and can be used for direct comparison with state of the art theoretical predictions, leading to advances in these approaches. There has been a large volume of work produced in this area, with some recent representative examples provided in references [1–8]. In this contribution we present photoelectron spectra of the halide-acetylene anion gas phase complexes, and accompanying ab initio calculations for the neutral halogen-acetylene complexes.

The anion halide-acetylene species have received prior experimental and theoretical attention, with the first published experimental data being from matrix infrared spectroscopy of acetylene co-deposited with caesium halide salts in an argon matrix [9]. The most intense bands observed in the spectra of $F^-\cdots C_2H_2$, $Cl^-\cdots C_2H_2$, and $I^-\cdots C_2H_2$ were located at 2873, 3050 and 3182 cm^{-1} and were assigned to the hydrogen bonded C-H stretch of a linear $X^-\cdots HCCH$ complex. There was also evidence of the free C-H stretching mode, confirming the linear bonding motif. Of course the vibrational frequencies reported in this study are potentially perturbed somewhat by the co-deposited Cs^+ ions and by interactions with the argon matrix.

A decade later, the first gas-phase infrared spectra were recorded for not only the halide-acetylene 1:1 complexes, however also for larger clusters of the form $X^-\cdots(C_2H_2)_n$ [10–14]. The gas-phase spectra allowed for refinement of the stretching frequency of the hydrogen bonded C-H group, while other notable outcomes were the prediction of the first solvation shell size for the bromide and chloride-acetylene clusters [11, 13] and partial rotational resolution in the infrared spectrum of $Br^-\cdots C_2H_2$ which allowed for the determination of a very accurate value for D_0; 3020(3) cm^{-1}[14]. Indeed, this was the first instance of resolved ΔJ structure in the infrared spectrum of a gas phase anion-molecule complex. There was an issue with the interpretation of the spectrum of the $Cl^-\cdots C_2H_2$, arising from the fact that vibrational predissociation spectroscopy was used to record the infrared spectrum and that the binding energy of the complex exceeded the energy of the H-bonded stretching mode. For this reason the observed infrared absorption was in fact a hot band transition, however a more reliable H-bonded C-H stretching frequency was determined after 'argon tagging' spectroscopy was utilised [15].

Turning our attention now to the prior theoretical work, the fluoride-acetylene complex was the first of these systems characterised in the mid 1980's using HF theory with the rather small 3-21+G and 4-31+G

basis sets [16, 17]. A linear complex geometry was predicted with a binding energy around 85 kJ mol^{-1}. The same complex was again investigated in the 1990's with MP2 single point energy calculations of an HF optimised geometry, using in this instance the 6-31+G* basis set. The predicted binding energy agreed with the earlier HF values. Other MP2 calculations were carried out in conjunction with the gas-phase infrared spectrum of the $Br^{-}\cdots C_2H_2$ complex, however these calculations were shown to be somewhat flawed by higher level calculations performed Botschwina and co-workers (vide infra) due to the MP2 treatment correlating all electrons while the valence-only correlation consistent aug-cc-pVTZ basis sets were utilised in the calculations [14]. Shortly after this study, Meuwly and co-workers performed ro-vibrational calculations for the $Cl^{-}\cdots C_2H_2$ complex on an adiabatically corrected MP2 potential energy surface, using Dunning's aug-cc-pVTZ basis sets [18].

The highest level calculations on the suite of halide-acetylene complexes have been performed by Botschwina and co-workers. They used the CCSD(T) methodology with the very large augmented correlation consistent basis sets of Dunning thereby furnishing very accurate structures and values for the binding energy, D_e [19–21]. In addition anharmonicity constants were determined for the stretching modes from variational calculations based on CCSD(T) stretch only potential energy surfaces.

To the best of our knowledge the analogous neutral halogen-acetylene species have been characterised neither by experiment nor theory. We therefore are in a position to perform high level ab initio calculations on these systems to determine the stationary points on the potential energy surface. We can critically assess the predicted structures and binding energies (D_0) for the neutral complexes through comparison with the experimental electron affinities afforded through photoelectron spectroscopy.

2 Methodology

2.1 Experimental Methods

The apparatus at UWA consists of a time of flight mass spectrometer for anion species based on the design of Wiley and McLaren [22] coupled to a magnetic bottle photoelectron spectrometer similar to that introduced by Cheshnovsky et al [23]. The design of the spectrometer has been described previously [24], and hence only those conditions relevant to the experiments on halide-acetylene complexes, or any recent modifications to the apparatus, are described here. The complexes were formed in a plasma created by intersecting energetic electrons with a pulsed supersonic expansion of a gas in a vacuum chamber. The electron source has been modified from that described in reference [24] and now includes a home built

miniature Einzel lens assembly which allows for the focussing of the electrons onto the gas expansion. The composition of the gas mixture is varied to produce the ion clusters of interest, and in the present study consists of a mixture of acetylene and argon (1:10 ratio) seeded with traces of CH_3I, CH_2Br_2, or CCl_4 (halide anion precursors). The total pressure of the gas mixture was 400 kPa. The $X^- \cdots C_2H_2$ clusters are selected using time of flight mass spectrometry and the cluster of choice is subsequently overlapped in the presence of a strongly divergent magnetic field by a 5 ns pulse of 266 nm radiation (4.66 eV, 4th harmonic of a Nd:YAG laser, Spectra Physics Quanta Ray Pro). The generated photoelectrons are guided to a detector at the end of a 1.5 m flight tube by means of a second homogeneous magnetic field subjected to the entire length of the flight tube. To improve the detection of low energy electrons, a grounded mesh is placed approximately 2 cm in front of the microchannel plate detector, and the front face of the detector is biased to +200 V. The time of flight of the detached photoelectrons with respect to the laser pulse is recorded and initially converted to kinetic energy (eKE). The electron binding energy (eBE) is then obtained using the following expression:

$$eBE = h\nu - eKE \tag{1}$$

where $h\nu$ is the energy of the incident photon (266 nm, 4.66 eV). In this fashion, the spectra represent transitions from anion states to the various neutral states and resemble conventional absorption spectra. Multiple spectra were recorded over several days and subsequently averaged for a given cluster. Each individual spectrum was collected over 10 000 laser shots. Calibration of the spectrometer was achieved by recording the spectra from the bare halide anions, thereby producing a calibration curve of known eKE versus electron TOF, and subsequently the Jacobi transformation ($dt \rightarrow dE$) was applied which corrects for the conversion from time of flight binning to energy binning of the photoelectrons. According to Cheshnovsky et al [23], the main influence on the resolution of a magnetic bottle photoelectron spectrometer is the velocity of the anion, with the spread in photoelectron energies is determined from,

$$dE_e = 4\sqrt{\frac{m_e}{m_I} E_e E_I} \tag{2}$$

where E_e and E_I denote the kinetic energies of the electron in the centre of mass and of the ion respectively, while m_e and m_I are the masses. As our spectrometer does not feature an ion decelerator, and the beam energy is 1000 eV, dE_e is 0.51 eV for an electron with 1.05 eV kinetic energy emitted from the chloride ion following absorption of a 4.66 eV photon. The resolution improves for larger ion masses with lower velocities, however we are limited to a minimum beam energy of 1000 eV.

2.2 Computational Methods

The halogen-acetylene neutral 1:1 complexes were investigated by ab initio calculations at the CCSD(T) level of theory with Dunning's triple zeta augmented correlation consistent basis set for carbon (aug-cc-pVTZ), for hydrogen the non-augmented basis set (cc-pVTZ), and for chlorine the aug-cc-pV(T+d)Z basis set with additional d-functions [25–27]. The aug-cc-pVTZ PP basis sets [28, 29] were employed for bromine and iodine as they greatly reduced the computation time and in addition they account for relativistic effects and consist of small-core relativistic pseudopotentials adjusted to multiconfiguration Dirac-Hartee-Fock data based on the Dirac-Coulomb-Breit Hamiltonian. The level of theory and basis set choice we have adopted is deemed to be appropriate as it has been used successfully in the description of the anion species by Botschwina and co-workers [19–21]. In addition, in order to ensure that our work is indeed consistent with that of Botschwina, we have undertaken calculations on the anion species for comparison.

For the open shell radical species the CCSD(T) calculations treated only the valence electrons, and were based on an unrestricted Hartree Fock (UHF) reference wavefunction. The geometries of the gas phase complexes were determined from the standard optimisation routines, with convergence criteria for the gradient being 1×10^{-8} hartree/bohr, which is deemed necessary considering the low binding energies of neutral van der Waals complexes, i.e. shallow and flat potential energy surfaces. Vibrational frequency analyses were performed at the located stationary points to determine whether they represented minima, transition states, or high order stationary points on the global potential energy surface. Energies of the bare neutral radicals, and the bare acetylene molecule were computed to aid in the determination of the binding energy D_e, and harmonic zero point energies of the complexes and bare acetylene were used to determine D_0. To improve upon the reliability of the predicted binding energies, we have employed single point energy calculations using up to quintuple-ζ basis sets, and subsequently performed a two point complete basis set limit extrapolation along the lines of W1 and W2 theory [30]. All quantum chemical calculations were performed using the CFOUR package [31].

Finally, anion photoelectron spectra were simulated by determining the Franck-Condon Factors (FCFs) linking the anion and neutral species vibrational states. FCFs were calculated using the ezSpectrum 3.0 program which is made freely available by Mozhayskiy and Krylov [32]. The program produces FCFs in either the parallel mode approximation as products of one-dimensional harmonic wavefunctions, or by undertaking Duschinsky rotations of the normal modes between states. The predicted stick spectra were convoluted with a Gaussian response function of width 0.002 eV to simulate an experimental high

resolution spectrum.

3 Results & Discussion

3.1 Computational Results

Two stationary points were located on the potential energy surface of halogen-acetylene gas phase complex corresponding to a linear $C_{\infty v}$ symmetry structure and the 'T-shaped' C_{2v} structure. Both structures are depicted in Figure 1, and pertinent geometrical parameters and binding energies are collected in Tables 1 and 2. Additional data on the complexes are provided in the supplementary information, including absolute electronic energies, vibrational mode frequencies, and zero point energies.

Table 1: *Structural parameters of the C_{2v} halogen-acetylene gas phase complexes predicted from CCSD(T)/a′pvtz calculations. D_e and D_0 are predicted using CCSD(T)/CBS results.*

	$r_{X\cdots\|\|\|}$*	r_{C-H}	$r_{C\equiv C}$	$\angle_{(X-\|\|\|-H)}$*	$\angle_{H-C-C}$	D_e	D_0	
	Å	Å	Å	°	°	kJ mol^{-1}	kJ mol^{-1}	cm^{-1}
Cl···HCCH	2.670	1.066	1.216	90.4	179.4	19.1	16.5	1379
Br···HCCH	2.855	1.066	1.214	90.4	179.4	18.2	17.0	1421
I···HCCH	3.188	1.066	1.213	90.2	179.6	17.3	16.3	1363
HCCH		1.065	1.210					

∗ ||| is the mid point of the C≡C bond

Table 2: *Structural parameters of the $C_{\infty v}$ halogen-acetylene gas phase complexes predicted from CCSD(T)/a′pvtz calculations. D_e and D_0 are predicted using CCSD(T)/CBS results.*

	$r_{H_b\cdots X}$	$r_{C_b-H_b}$	$r_{C\equiv C}$	$r_{C_a-H_a}$	D_e	D_0	
	Å	Å	Å	Å	kJ mol^{-1}	kJ mol^{-1}	cm^{-1}
Cl···HCCH	2.916	1.066	1.211	1.065	3.1	2.2	184
Br···HCCH	2.987	1.066	1.211	1.065	3.8	2.9	242
I···HCCH	3.190	1.066	1.211	1.065	5.5	4.7	393
HCCH		1.065	1.210	1.065			

As indicated earlier, to ensure that our computational approach is valid we have applied the methodology to the analogous anion halide-acetylene complexes and subsequently compared these results with those

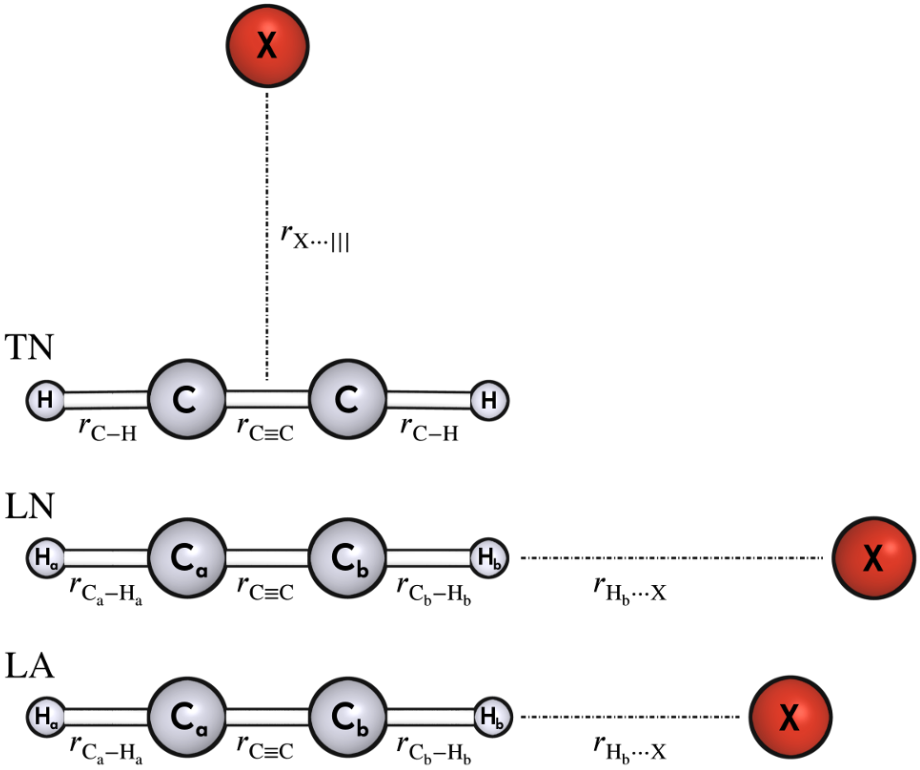

Figure 1: *Predicted stationary points for the neutral and anion halogen-acetylene complexes. TN is a T-shaped C_{2v} symmetry neutral geometry, LN is a linear $C_{\infty v}$ symmetry neutral geometry, and LA is a linear $C_{\infty v}$ symmetry anion geometry. Structural parameters are provided in Tables 1 to 3*

of Botschwina and co-workers [19–21]. The comparison is shown in Table 3, with the largest deviation in structural parameters seen for the Br$\cdots$HCCH separation, which is only 0.026 Å shorter in our work. Similarly, the cluster binding energies compare well, giving us confidence in applying the methodology to the neutral halogen-acetylene systems.

Returning now to the neutral halogen-acetylene complexes, the perturbing effect of the halogen radical on the acetylene unit is actually quite small, which is evident when one compares the geometric parameters of the complexed and free acetylene moiety (computed at the same level of theory, with the bare acetylene data provided in Tables 1 to 3). The largest difference in bond length is observed for the C−C bond in the Cl$\cdots$HCCH C_{2v} complex (TN in Figure 1), while there is also a small decrease in the H−C−C bond

Table 3: *Structural parameters of the $C_{\infty v}$ anion halide-acetylene gas phase complexes predicted from CCSD(T)/a′pvtz calculations. D_e and D_0 are predicted using CCSD(T)/CBS results.*

		$r_{H_b\cdots X}$ Å	$r_{C_b\cdots H_b}$ Å	$r_{C\equiv C}$ Å	$r_{C_a\cdots H_a}$ Å	D_e kJ mol^{-1}	D_0 kJ mol^{-1}	D_0 cm^{-1}
$Cl^-\cdots$HCCH	*This work*	2.258	1.093	1.216	1.064	45.1	43.2	3611
	Reference [20]	2.2521	1.0919	1.2118	1.0623			3600(36)
$Br^-\cdots$HCCH	*This work*	2.454	1.085	1.216	1.064	39.1	37.3	3188
	Reference [21]	2.4800	1.0860	1.2117	1.0627			3020(3)∗
$I^-\cdots$HCCH	*This work*	2.774	1.082	1.215	1.064	32.7	31.0	2591
	Reference [21]	2.7626	1.0809	1.2108	1.0626			2450(74)
HCCH			1.065	1.210	1.065			

∗ Experimental value from reference [14]

angles such that the hydrogen atoms point slightly towards the halogen. This angle changes from 180.0° to 179.4° for Cl$\cdots$HCCH and Br$\cdots$HCCH, and 179.6° for I$\cdots$HCCH. These small perturbations are indicative of the weak intermolecular interaction, which is further confirmed when one considers that the predicted cluster binding energies are all below 18 kJ mol^{-1}.

The predicted binding energies of the complexes, D_e, were determined from a two-point extrapolation of single point energies calculated using the larger aug-cc-pVQZ and aug-cc-pV5Z basis sets (PP varieties in the case of Br and I). Estimates for D_0 were determined using the zero point energies from aug-cc-pVTZ basis sets (again, cc-pVTZ for H, aug-cc-pV(T+d)Z for Cl and aug-cc-pVTZ PP in the case of Br and I). The trend for the linear complexes is an increase in D_0 for increasing halogen size, being 2.2, 2.9 and 4.7 kJ mol^{-1} for Cl, Br, and I respectively. For the C_{2v} symmetry complex, the predicted binding energies do not follow a trend, with D_0 for the Cl and I complex being quite close at 16.5 and 16.3 kJ mol^{-1} while for the Br species, D_0 is larger at 17.0 kJ mol^{-1}.

One can rationalise the trend in the cluster binding energies of the linear complexes, or lack thereof in the T-shaped complexes, by considering that the attractive interaction is due to dispersion, and hence is determined by the polarisabilities of the species involved. The dipole polarisabilities of the neutral halogens are 14.7, 21.8 and 34.6 au (where au $\equiv e^2 {a_0}^2 E_h^{-1}$) for chlorine, bromine, and iodine respectively [33, 34], while for acetylene there exists quite a large polarizability anisotropy whereby $\alpha_\perp$=18.66 au and $\alpha_\parallel$=30.2 au [35]. There will also be a decrease in the closeness of approach for the halogen to the carbon atoms, upon increased halogen size.

For the C_{2v} complexes, the balance between the attractive dispersion interaction and the closeness of approach comes into play, especially considering that the larger carbon atoms are presented to the halogens in this geometry. As the halogen size increases there is an increase in the dispersion interaction following the increased polarisability of the halogen, however this is offset by the increase in distance to which the halogen can approach due to the atomic radius. The end result is that the binding strength is largest for bromine, and drops off for the other two halogens depending on the balance of the two effects. For chlorine the polarisability is smaller than for bromine, and for iodine although the polarisability is larger the distance to the the acetylene is larger leading to a smaller interaction.

When one considers the linear $C_{\infty v}$ complex, the halogen is situated close to the much smaller hydrogen, and hence is not precluded from approaching as in the T-shaped case where the halogen is presented to the two carbon atoms. While the dispersion interaction is small, leading to low interaction energies, the hydrogen does not restrict access as much as the carbon atoms. The trend of increasing binding energy is therefore dominated by the increased polarisability of the halogen.

3.1.1 Predicted Photoelectron Spectra

Armed with the predicted electronic and zero point energies of the anion and neutral complexes, we are in a position to predict the adiabatic detachment energy (ADE). We also computed the vertical detachment energies for the anion complexes by performing a neutral single point energy calculation for the complex at the anion geometry. In all cases the predicted vertical detachment energy lay below the predicted adiabatic detachment energ (these data are provided in the electronic supplementary information). For this reason, the adiabatic detachment energy is used in the simulations below.

We should note that the predicted ADEs do not take into account the spin-orbit splitting of the neutral halogen states, and these were accounted for by including the known spin-orbit coupling constants to split the predicted transition into two components, corresponding to the $^2P_{3/2} \leftarrow {}^1S_0$ and $^2P_{1/2} \leftarrow {}^1S_0$ transitions [36, 37]. Furthermore, to account for errors introduced by the CCSD(T) level of theory we apply a second shift which is determined by the differences in the predicted detachment energy of the bare halogen anions, and the known experimental values. These data are provided in the supplementary material. The correction decreases upon increased basis set size, and is small when the CBS limit extrapolated single point energies are compared with experiment. For chloride, bromide, and iodide the corrections are -0.015, 0.006 and 0.000 eV, respectively. the predicted adiabatic detachment energy from the anion to each of the neutral minima are provided in Table 4, and will be discussed later in reference to the experimental spectra.

A representative predicted photoelectron spectrum for the $I^-\cdots HCCH$ complex is shown in Figure 2. The spectrum was produced from the geometries (Figure 1 and Tables 2 and 3), vibrational frequencies, and vibrational normal mode coordinates. This procedure is possible for the linear $C_{\infty v}$ complexes, however not for the anion to C_{2v} T-shaped neutral as the geometry change is too large. All simulations were performed at a temperature which is characteristic of a supersonic molecular beam, i.e. vibrational temperatures of around 20 K, and we allowed for 5 quanta of excitation in each vibrational mode of the anion complex, and up to 10 quanta for the neutral complex. A full set of these data, incorporating transition energies, intensities, Franck-Condon Factors, and transition assignments, are available in the electronic supplementary material.

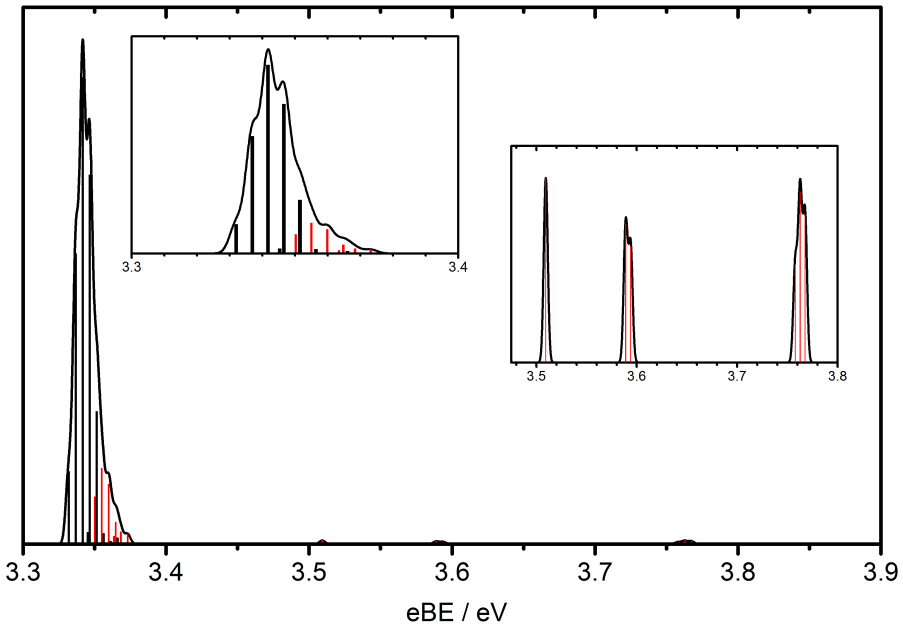

Figure 2: *Predicted anion photoelectrum spectrum of the $I^-\cdots HCCH$ complex. The insets show regions of the spectrum on expanded scales.*

Looking to Figure 2, the main band of the predicted photoelectron spectrum has been shifted such that the $0 \leftarrow 0$ transition is at the predicted adiabatic detachment energy in Table 4. The major progression predicted (black stick spectrum in Figure 2) is associated with the intermolecular stretching mode. This is expected considering that the intermolecular separation between iodide and HCCH changes from 2.774 Å in the anion to 3.190 Å for the neutral. Indeed the most intense transition corresponds to the $v'' = 0$ to $v' = 2$ transition in the intermolecular stretching mode. The smaller progression is built on a combination of the intermolecular stretch, and two quanta of the intermolecular bend. Weaker bands are predicted at higher electron binding energy and are based on the C−H stretch modes. These again arise from the

structural differences between anion and neutral complexes, especially the C-H bond associated with the hydrogen in close proximity to the halogen, which using the iodine complexes as an example decreases from 1.082 Å in the anion complex to 1.066 Å in the neutral (refer to Tables 2 and 3).

The main predicted photoelectron band for all three complexes is shown in Figure 3. The differences arise from variations in the intermolecular stretch frequency, with the most noticeable variation for the $I^- \cdots$ HCCH complex.

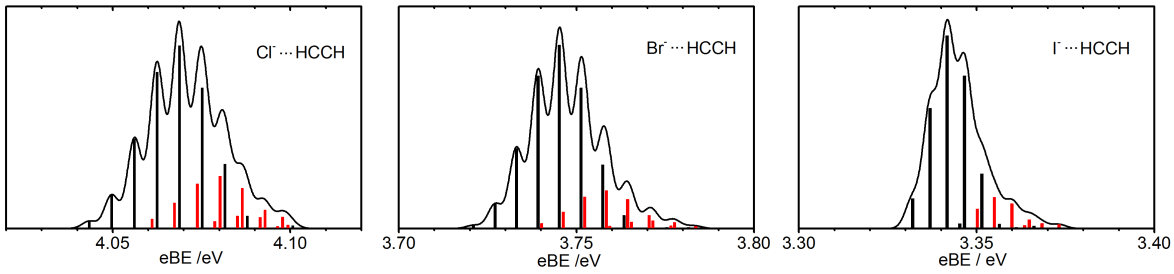

Figure 3: *Predicted anion photoelectron spectra of the $X^- \cdots$ HCCH complexes, where $X^- = Cl^-$, Br^-, and I^-. The black stick spectra correspond to the progression in the intermolecular stretching mode, while the red stick spectra are combination bands.*

3.2 Experimental Photoelectron spectra

The experimental photoelectron spectra for the halide-acetylene complexes, recorded using 266 nm radiation (4.66 eV) are shown in Figure 4. Data derived from the spectra are provided in Table 4, and consist of peak positions and stabilisation energies. The spectra do not show vibrational progressions due to the low resolution of our spectrometer, however they do reveal quite a large shift in the electron binding energies upon complex formation. Aside from this shift, the fact that the spectra of each complex closely resembles the bare anion is clear evidence for a non-covalent interaction, whereby the spectrum is best considered to be that of the halide anion perturbed by the solvating acetylene. Considering the degeneracy of the two spin orbit states of the neutral halogen, the ratio of the peak intensities should be 2:1 ($^2P_{3/2}$:$^2P_{1/2}$), however due to a decrease in detection efficiency for slow electrons in our apparatus, the $^2P_{1/2}$ component has somewhat reduced intensity.

Formation of the complex between the halogen anions and acetylene results in the observed shift of the two spin orbit states to higher electron binding energy (eBE) compared to the bare halide anions, while the separation between the states remains constant. The shift to higher energy is a direct result of

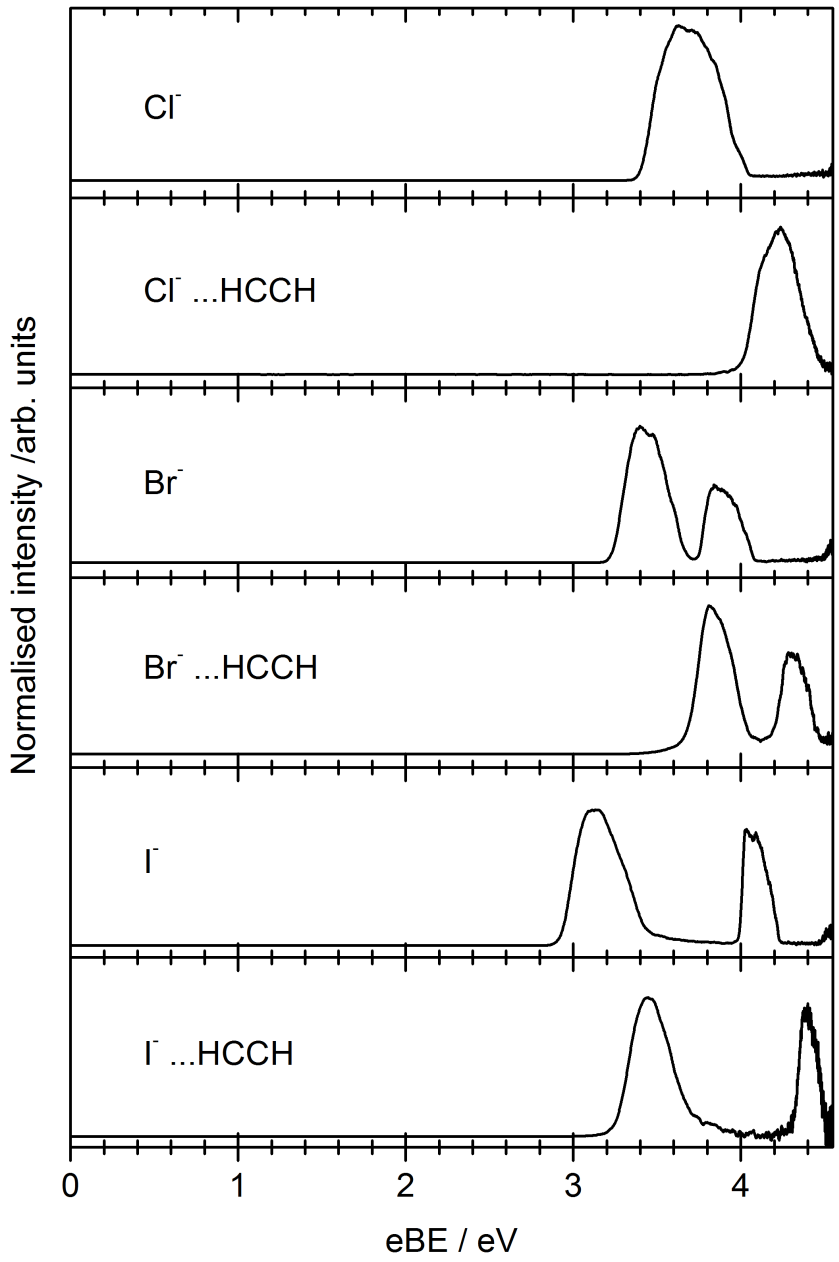

Figure 4: *Anion photoelectron spectra of the halide-acetylene gas phase complexes, recorded with photon energy 4.66 eV.*

the stabilisation of the anion afforded through complex formation with the acetylene molecule, or more precisely is due to the difference in the dissociation energies of the anion and neutral complexes. If D_0 were the same for both complexes then the result would be no shift of the photoelectron band compared

with the bare X^- anions. As seen from the ab initio predictions, the neutral complexes have a smaller D_0 as they are bound by dispersion forces only, while for the anion complex there are additional electrostatic charge-quadrupole and charge-induced dipole interactions. As an example of the disparity in binding energies, the $Cl^- \cdots HCCH$ anion complex binding energy is predicted to be $D_0 = 43.2\,kJ\,mol^{-1}$ while it is $16.5\,kJ\,mol^{-1}$ and $2.2\,kJ\,mol^{-1}$ for the C_{2v} and $C_{\infty v}$ neutral complexes, respectively (Tables 1 and 2, CCSD(T)/CBS limit extrapolation results).

Table 4: *Experimental photoelectron band positions. Also included are the predicted adiabatic detachment energy to the $^2P_{3/2}$ from CCSD(T)/CBS calculations, see text for details. Uncertainties represent the 95% CI, determined by averaging band positions from multiple spectra.*

Species	$^2P_{3/2}$ eV	$^2P_{1/2}$ eV	E_{stab} meV	ADE $C_{\infty v}$ eV	ADE C_{2v} eV
Cl^-	3.6(4)				
$Cl^- \cdots HCCH$	4.1(1)		0.5	4.037	3.889
Br^-	3.39(6)	3.85(3)			
$Br^- \cdots HCCH$	3.806(8)	4.277(6)	0.41	3.721	3.574
I^-	3.05(4)	4.02(6)			
$I^- \cdots HCCH$	3.426(6)	4.37(4)	0.378	3.332	3.212

Comparing now the predicted adiabatic detachment energies for the complexes, the comparison is much better for the transition from anion to the linear $C_{\infty v}$ complex. This seems reasonable seeing the anion geometry most resembles the linear neutral geometry.

3.2.1 Comparison with other halide-molecule complexes

We conclude by comparing the electron affinities and stabilisation energies of the $X \cdots HCCH$ complexes with other similar halogen-molecule species. In the first instance we note that the stabilisation energies decrease down the halide series, which is again due to the smaller dissociation energies for the anion complexes upon increased halogen size. Referring to Table 3 the predicted binding energies at the CCSD(T)/CBS limit are 43.2, 37.3 and $31.0\,kJ\,mol^{-1}$, while from Table 4 the stabilisation energies are 0.5, 0.41 and 0.38 eV. The stabilisation energy correlates strongly with the dissociation energy (D_0) of the anion-molecule complex due to the fact that D_0 is much larger for the anion compared with the neutral.

When compared to other complexes investigated previously by our group, i.e. the halide-carbon monoxide species, the halide-acetylene set display much larger stabilisation energies, which is to be expected

considering that the predicted D_0 values are 14.6, 9.9 and 7.3 kJ mol^{-1} for the chloride, bromide, and iodide-carbon monoxide complexes respectively, while the stabilisation energies are 0.16, 0.14 and 0.09 eV [24, 38, 39]. In the present case the anion is bound via hydrogen bonding, whereas for the carbon monoxide systems the interaction is somewhat weaker and is primarily the charge-quadrupole interaction seeing carbon monoxide has a relatively small dipole moment.

Finally, it is interesting to compare the stabilisation energies of the halide-acetylene complexes with those of another series bound by hydrogen bonding, namely the halide-water complexes. The current results are on a par with the halide-water stabilisation energies, being 0.76, 0.55 and 0.45 eV [40] which is a consequence of similar anion complex binding energies, i.e. 62.3, 51.5 and 43.0 kJ mol^{-1} for chloride, bromide, and iodide-water complexes respectively [36]. These data are not strictly D_0, however rather the enthalpy of ligand association $\Delta_r H$.

4 Summary

Experimental photoelectron spectra were recorded for the halide-acetylene dimer complexes. The spectral features shift to higher electron binding energy which is a result of the larger binding energy of the anion cluster compared with its neutral analogue. The spectra are unfortunately devoid of vibrational resolution, however we are able to determine electron detachment energies, and hence electron affinities for the neutral complexes. Ab initio calculations performed at CCSD(T) level of theory were used to predict structures for the neutral dimer complexes. Two minima were predicted to exist, corresponding to a T-shaped geometry of C_{2v} symmetry, and a linear $C_{\infty v}$ symmetry complex. Both are loosely bound, with binding energies less than 18 kJ mol^{-1}. The predicted electron detachment energies for detachment from the linear anion complex to the linear neutral complex compares very well with experiment.

5 Acknowledgements

KLM and MK acknowledge the support of an Australian Postgraduate Award (APA). We acknowledge financial support from the Faculty of Science and the School of Chemistry and Biochemistry, and the Australian Research Council is acknowledged for funding under the LIEF scheme (LE110100093). Prof Mark Spackman and Dr Amir Karton are acknowledged for fruitful discussions on intermolecular interactions and complete basis set limit extrapolation respectively.

References

[1] B. Opoku-Agyeman, A. Case, J. H. Lehman, W. C. Lineberger, and A. McCoy. "Nonadiabatic photofragmentation dynamics of BrCN-". In: *Journal of Chemical Physics* 141 (2014), p. 084305. DOI: 10.1063/1.4892981.

[2] J. P. Martin, A. Case, Q. L. Gu, J. P. Darr, A. B. McCoy, and W. C. Lineberger. "Photofragmentation dynamics of ICN−$(CO_2)_n$ clusters following visible excitation". In: *Journal of Chemical Physics* 139 (2013), p. 064315. DOI: 10.1063/1.4817664.

[3] J. B. Kim, M. L. Weichman, and D. M. Neumark. "Structural Isomers of Ti_2O_4 and Zr_2O_4 Anions Identified by Slow Photoelectron Velocity-Map Imaging Spectroscopy". In: *Journal of the American Chemical Society* 136 (2014), pp. 7159–7168. DOI: 10.1021/ja502713v.

[4] M. L. Weichman, J. B. Kim, and D. M. Neumark. "Rovibronic structure in slow photoelectron velocity-map imaging spectroscopy of CH_2CN^- and CD_2CN^-". In: *Journal of Chemical Physics* 140 (2014), p. 104305. DOI: 10.1063/1.4867501.

[5] J. D. Graham, A. M. Buytendyk, X. Zhang, E. L. Collins, B. Kiran, G. Gantefoer, B. W. Eichhorn, G. L. Gutsev, S. Behera, et al. "Alanate Anion, AlH_4^-: Photoelectron Spectrum and Computations". In: *Journal of Physical Chemistry A* 118 (2014), pp. 8158–8162. DOI: 10.1021/jp500678n.

[6] A. Buytendyk, J. Graham, H. P. Wang, X. X. Zhang, E. Collins, Y. J. Ko, G. Gantefoer, B. Eichhorn, A. Regmi, et al. "Photoelectron spectra of the MgH- and MgD- anions". In: *International Jounral of Mass Spectrometry* 365 (2014), pp. 140–142. DOI: 10.1016/j.ijms.2013.12.017.

[7] I. A. Popov, W. L. Li, Z. A. Piazza, A. I. Boldyrev, and L. S. Wang. "Complexes between Planar Boron Clusters and Transition Metals: A Photoelectron Spectroscopy and Ab Initio Study of CoB_{12}^- and RhB_{12}^-". In: *Journal of Physical Chemistry A* 118 (2014), pp. 8098–8105. DOI: 10.1021/jp411867q.

[8] Y. Erdogdu, T. Jian, G. V. Lopez, W. L. Li, and L. S. Wang. "On the electronic structure and chemical bonding of titanium tetraauride: $TiAu_4$ and $TiAu_4^-$". In: *Chemical Physics Letters* 610 (2014), pp. 23–28. DOI: 10.1016/j.cplett.2014.07.018.

[9] M. L. H. Jeng and B. S. Ault. "Infrared matrix isolation studies of molecular interactions: alkynes with halide anions". In: *Journal of Physical Chemistry A* 95 (1991), pp. 2687–2692. DOI: 10.1021/j100160a013.

[10] P. S. Weiser, D. A. Wild, and E. J. Bieske. "Infrared Spectra of $I^-(C_2H_2)_n$ ($1 \leq n \leq 4$) anion complexes". In: *Chemical Physics Letters* 299 (1999), pp. 303–308. DOI: 10.1016/S0009-2614(98)01286-X.

[11] P. S. Weiser, D. A. Wild, and E. J. Bieske. "Infrared Spectra of $Cl^-(C_2H_2)_n$ ($1 \leq n \leq 9$) anion clusters: Spectroscopic evidence for solvent chell closure". In: *Journal of Chemical Physics* 110 (1999), pp. 9443–9449. DOI: 10.1063/1.478909.

[12] D. A. Wild, Z. M. Loh, and E. J. Bieske. "Infrared Spectra and ab initio Calculations for Fluoride-acetylene Clusters: $F^-(HCCH)_n$, $n = 3 - 6$". In: *The Australian Journal of Chemistry* 64 (2011), pp. 633–637. DOI: 10.1071/CH11032.

[13] D. A. Wild, P. J. Milley, Z. M. Loh, P. Weiser, and E. Bieske. "Infrared spectra of $Br^-(C_2H_2)_n$ complexes". In: *Chemical Physics Letters* 323 (2000), pp. 49–54. DOI: 10.1016/S0009-2614(00)00465-6.

[14] D. A. Wild, P. J. Milley, Z. M. Loh, P. P. Wolynec, P. S. Weiser, and E. J. Bieske. "Structural and energetic properties of the $Br^-C_2H_2$ anion complex from rotationally resolved mid-infrared spectra and ab initio calculations". In: *Journal of Chemical Physics* 113 (2000), pp. 1075–1080. DOI: 10.1063/1.481919.

[15] D. A. Wild, Z. M. Loh, R. L. Wilson, and E. J. Bieske. "Locating and confirming the C–H stretch bands of the halide–acetylene anion complexes using argon predissociation spectroscopy". In: *Chemical Physics Letters* 369 (2003), pp. 684–690. DOI: 10.1016/S0009-2614(03)00038-1.

[16] P. v. R. Schleyer and A. J. Kos. "The importance of negative (anionic) hyperconjugation". In: *Tetrahedron* 39 (1983), pp. 1141–1150. DOI: 10.1016/S0040-4020(01)91877-0.

[17] M. Roy and T. B. McMahon. "The anomalous gas phase acidity of ethyl fluoride. An ab initio investigation of the importance of hydrogen bonding between F^- and sp^2 and sp C-H bonds". In: *Canadian Journal of Chemistry* 63 (1985), pp. 708–715. DOI: 10.1139/v85-117.

[18] M. Meuwly, P. P. Wolynec, and E. J. Bieske. "Potential energy surface and lower bound states of $HCCH-Cl^-$". In: *Journal of Chemical Physics* 116 (2002), pp. 4948–4954. DOI: 10.1063/1.1449870.

[19] P. Botschwina, T. Dutoi, M. Mladenović, R. Oswald, S. Schmatz, and H. Stoll. "Theoretical investigations of proton-bound cluster ions". In: *Faraday Discussions* 118 (2001), pp. 433–453. DOI: 10.1039/b010076p.

[20] P. Botschwina and R. Oswald. “The anionic complex Cl^-. . . HCCH: Results of large-scale coupled cluster calculations”. In: *Journal of Chemical Physics* 117 (2002), pp. 4800–4802. DOI: 10.1063/1.1497643.

[21] P. Botschwina and H. Stoll. “The hydrogen-bonded cluster anions Br^-. . . HCCH and I^-. . . HCCH: results of coupled cluster calculations”. In: *Physical Chemistry Chemical Physics* 3 (2001), pp. 1965–1972. DOI: 10.1039/b100549i.

[22] W. C. Wiley and I. H. McLaren. “Time of Flight Mass Spectrometer with Improved Resolution”. In: *Review of Scientific Instruments* 26 (1955), pp. 1150–1157. DOI: 10.1063/1.1715212.

[23] O. Cheshnovsky, S. H. Yang, C. L. Pettiette, M. J. Craycraft, and R. E. Smalley. “Magnetic time-of-flight photoelectron spectrometer for mass-selected negative cluster ions”. In: *Review of Scientific Instruments* 58 (1987), pp. 2131–2137. DOI: 10.1063/1.1139475.

[24] K. Lapere, R. LaMacchia, L. Quak, A. McKinley, and D. Wild. “Anion photoelectron spectroscopy and ab initio calculations of the gas phase chloride–carbon monoxide complex: Cl^-. . . CO”. In: *Chemical Physics Letters* 504 (2011), pp. 13–19. DOI: 10.1016/j.cplett.2011.01.034.

[25] T. H. Dunning Jr. “Gaussian basis sets for use in correlated molecular calculations. I. The atoms boron through neon and hydrogen”. In: *Journal of Chemical Physics* 90 (1989), p. 1007. DOI: 10.1063/1.456153.

[26] D. E. Woon and T. H. Dunning Jr. “Gaussian basis sets for use in correlated molecular calculations. III. The atoms aluminum through argon”. In: *Journal of Chemical Physics* 98 (1993), p. 1358. DOI: 10.1063/1.464303.

[27] T. H. Dunning Jr., K. A. Peterson, and A. K. Wilson. “Gaussian basis sets for use in correlated molecular calculations. X. The atoms aluminum through argon revisited”. In: *Journal of Chemical Physics* 114 (2001), p. 9244. DOI: 10.1063/1.1367373.

[28] K. A. Peterson, D. Figgern, E. Goll, H. Stoll, and M. Dolg. “Systematically convergent basis sets with relativistic pseudopotentials. II. Small-core pseudopotentials and correlation consistent basis sets for the post-d group 16–18 elements”. In: *Journal of Chemical Physics* 119 (2003), p. 11113. DOI: 10.1063/1.1622924.

[29] K. A. Peterson, B. C. Shepler, D. Figgen, and H. Stoll. “On the spectroscopic and thermochemical properties of ClO, BrO, IO, and their anions”. In: *Journal of Physical Chemistry A* 110 (2006), pp. 13877–13883. DOI: 10.1021/jp065887l.

[30] A. Karton and J. M. Martin. “Explicitly correlated Wn theory: W1-F12 and W2-F12”. In: *Journal of Chemical Physics* 136 (2012), p. 124114. DOI: 10.1063/1.3697678.

[31] CFOUR, a quantum chemical program package written by J.F. Stanton, J. Gauss, M.E. Harding, P.G. Szalay with contributions from A.A. Auer, R.J. Bartlett, U. Benedikt, C. Berger, D.E. Bernholdt, Y.J. Bomble, O. Christiansen, M. Heckert, O. Heun, C. Huber, T.-C. Jagau, D. Jonsson, J. Jusélius, K. Klein, W.J. Lauderdale, D.A. Matthews, T. Metzroth, D.P. O’Neill, D.R. Price, E. Prochnow, K. Ruud, F. Schiffmann, S. Stopkowicz, A. Tajti, J. Vázquez, F. Wang, J.D. Watts and the integral packages MOLECULE (J. Almlöf and P.R. Taylor), PROPS (P.R. Taylor), ABACUS (T. Helgaker, H.J. Aa. Jensen, P. Jørgensen, and J. Olsen), and ECP routines by A. V. Mitin and C. van Wüllen. For the current version, see http://www.cfour.de.

[32] V. A. Mozhayskiy and A. I. Krylov. *ezSpectrum 3.0*. 2009. URL: http://iopenshell.usc.edu/downloads.

[33] E. A. Reinsch and W. Meyer. “Finite perturbation calculation for the static dipole polarizabilities of the atoms Na through Ca”. In: *Physical Review A* 14 (1976), pp. 915–918. DOI: 10.1103/PhysRevA.14.915.

[34] T. Fleiq and A. J. Sadlej. “Electric dipole polarizabilities of the halogen atoms in $^2P_{1/2}$ and $^2P_{3/2}$ states: Scalar relativistic and two-component configuration-interaction calculations”. In: *Physical Review A* 65 (2002), p. 032506. DOI: 10.1103/PhysRevA.65.032506.

[35] G. Maroulis and A. J. Thakkar. “How important is electron correlation for the hyperpolarizability of ethyne”. In: *Journal of Chemical Physics* 93 (2002), p. 652. DOI: 10.1063/1.459512.

[36] National Institute of Standards and Technology, 2002, NIST Chemistry WebBook NIST Standard Reference Database Number 69, Gaithersburg, MD: NIST.

[37] National Institute of Standards and Technology, 2003, Handbook of Basic Atomic Spectroscopic Data, NIST Standard Reference Database 108, Gaithersburg, MD: NIST.

[38] K. M. Lapere, R. J. LaMacchia, L. H. Quak, M. Kettner, S. G. Dale, A. J. McKinley, and D. A. Wild. “The Bromide–Carbon Monoxide Gas Phase Complex: Anion Photoelectron Spectroscopy and Ab Initio Calculations”. In: *Australia Journal of Chemistry* 65 (2012), pp. 457–462. DOI: 10.1071/CH12007.

[39] K. M. Lapere, R. J. LaMacchia, L. H. Quak, M. Kettner, S. G. Dale, A. J. McKinley, and D. A. Wild. “Anion photoelectron spectra and ab initio calculations of the iodide carbon monoxide

clusters: $I^- \cdots (CO)_n$, n=1-4". In: *Journal of Physical Chemistry A* 116 (2012), pp. 3577–3584. DOI: 10.1021/jp300471x.

[40] G. Markovich, S. Pollack, R. Giniger, and O. Cheshnovsky. "Photoelectron spectroscopy of Cl^-, Br^-, and I^- solvated in water clusters". In: *Journal of Chemical Physics* 101 (1994), p. 11. DOI: 10.1063/1.467965.

6 Electronic Supporting Information

Table S1: *Structural parameters of the C_{2v} halogen-acetylene gas phase complexes predicted from CCSD(T) calculations*

		$r_{X\cdots\vert\vert\vert}$*	r_{C-H}	$r_{C\equiv C}$	$\angle_{(X-\vert\vert\vert-H)}$	$\angle_{H-C-C}$	$E_{CCSD(T)}$	zpe	D_e	D_0		ADE
		Å	Å	Å	°	°	E_h	kJ mol^{-1}	kJ mol^{-1}	kJ mol^{-1}	cm^{-1}	eV
Cl···HCCH	a′pvtz	2.670	1.066	1.216	90.4	179.4	-536.875556	71.9	16.5	13.9	1162	3.806
	a′pvqz	2.638	1.065	1.213	90.4	179.3	-536.913507	72.3	17.9	15.2	1271	3.893
	a′pvtz//qz						-536.913463					
	a′pvtz//5z						-536.924666					
	CBS						-536.935594		19.1	16.5	1379	3.940
												3.889 & 3.998 †
Br···HCCH	a′pvtz	2.855	1.066	1.214	90.4	179.4	-492.911202	70.5	17.1	15.8	1321	3.576
	a′pvtz//qz						-493.003175					
	a′pvtz//5z						-493.086340					
	CBS						-493.172974		18.2	17.0	1421	3.732
												3.574 & 4.031 †
I···HCCH	a′pvtz	3.188	1.066	1.213	90.2	179.6	-372.062407	70.3	14.7	13.6	1137	3.350
	a′pvtz//qz						-372.156848					
	a′pvtz//5z						-372.216574					
	CBS						-372.278626		17.3	16.3	1363	3.527
												3.212 & 4.155 †

∗ ||| is the mid point of the C≡C bond

† CCSD(T)/CBS results split by experimental spin-orbit splitting, and shifted by factor in Table S4

Table S2: *Structural parameters of the $C_{\infty v}$ halogen-acetylene gas phase complexes predicted from CCSD(T) calculations*

		$r_{H_b\cdots X}$	$r_{C_b-H_b}$	$r_{C\equiv C}$	$r_{C_a-H_a}$	$\angle_{X-H-C}$	$E_{CCSD(T)}$	zpe	D_e	D_0		ΔE	ADE
		Å	Å	Å	°	°	E_h	kJ mol^{-1}	kJ mol^{-1}	kJ mol^{-1}	cm^{-1}	kJ mol^{-1}	eV
Cl$\cdots$HCCH	a′pvtz	2.916	1.066	1.211	1.065	180.0	-536.870541	70.2	3.3	2.4	201	11.4	3.952
	a′pvqz	2.903	1.065	1.201	1.064	180.0	-536.907905	70.3	3.2	2.5	209	12.7	4.025
	a′pvtz//qz						-536.907879						
	a′pvtz//5z						-536.918840						
	CBS						-536.929508		3.1	2.2	184		4.088
													4.037 & 4.146 ∗
Br$\cdots$HCCH	a′pvtz	2.987	1.066	1.211	1.065	180.0	-492.906432	70.3	4.6	3.5	293	12.3	3.704
	a′pvtz//qz						-492.997883						
	a′pvtz//5z						-493.080982						
	CBS						-493.167500		3.9	2.9	242		3.879
													3.721 & 4.178 ∗
Br$\cdots$HCCH	a′pvtz	3.190	1.066	1.211	1.065	180.0	-372.058766	70.1	5.1	4.3	360	9.2	3.447
	a′pvtz//qz						-372.152741						
	a′pvtz//5z						-372.212270						
	CBS						-372.274110		5.5	4.7	393		3.647
													3.332 & 4.275 ∗

∗ CCSD(T)/CBS results split by experimental spin-orbit splitting, and shifted by factor in Table S4

Table S3: *Structural parameters of the $C_{\infty v}$ halide-acetylene gas phase complexes predicted from CCSD(T) calculations*

		$r_{H_b\cdots X}$	$r_{C_b-H_b}$	$r_{C\equiv C}$	$r_{C_a-H_a}$	$\angle_{X-H-C}$	$E_{CCSD(T)}$	zpe	D_e	D_0		$E_{neutral}$	VDE
		Å	Å	Å	°	°	E_h	kJ mol^{-1}	kJ mol^{-1}	kJ mol^{-1}	cm^{-1}	E_h	eV
$Cl^-\cdots$HCCH	a′pvtz	2.258	1.093	1.216	1.064	180.0	-537.015146	71.2	44.9	43.1	3602	-536.866564	3.305
	a′pvqz	2.260	1.092	1.213	1.063	180.0	-537.056286	71.5	44.8	43.0	3595	-536.902708	3.437
	a′pvtz//qz						-537.056261						
	a′pvtz//5z						-537.068293						
	CBS						-537.080131		45.1	43.2	3611		
	Ref	2.2521	1.0919	1.2118	1.0623	180.0					3600(36)		
$Br^-\cdots$HCCH	a′pvtz	2.454	1.085	1.216	1.064	180.0	-493.042871	71.1	39.5	37.6	3143	-492.904009	3.041
	a′pvtz//qz						-493.138221						
	a′pvtz//5z						-493.222510						
	CBS						-493.310364		39.1	37.3	3118		
	Ref	2.4800	1.0860	1.2117	1.0627	180.0					3020(3)∗		
$I^-\cdots$HCCH	a′pvtz	2.774	1.082	1.215	1.064	180.0	-372.185793	71.0	31.8	30.0	2507	-372.057541	2.753
	a′pvtz//qz						-372.284311						
	a′pvtz//5z						-372.345182						
	CBS						-372.408492		32.7	31.0	2591		
	Ref	2.7626	1.0809	1.2108	1.0626	180.0					2450(74)		

∗ Experimental value from predissociation spectroscopy, reference [14]

Table S4: *Structural parameters and energies of bare acetylene, bare anions, and bare radicals predicted from CCSD(T) calculations*

		r_{H-C}	$r_{C\equiv C}$	$E_{CCSD(T)}$	zpe	VDE	Exp. SO ∗	Split	Literature $^2P_{3/2}$ VDE †	Shift ‡
		Å	Å	E_h	kJ mol^{-1}	eV	eV	eV	eV	eV
HCCH	a′pvtz	1.065	1.210	-77.191414	69.3					
	a′pvqz	1.065	1.207	-77.210794	69.6					
	a′pvtz//qz			-77.210768						
	a′pvtz//5z			-77.216332						
	CBS			-77.221621						
Cl^- | Cl	a′pvtz			-459.806626 | -459.677858		3.504	-0.036 | +0.073	3.468 | 3.577	3.613	+0.145
	a′pvqz			-459.828395 | -459.695891		3.606		3.570 | 3.679		+0.043
	a′pv5z			-459.834835 | -459.701313		3.633		3.597 | 3.706		+0.016
	CBS			-459.841344 | -459.706710		3.664		3.628 | 3.737		-0.015
Br^- | Br	a′pvtz			-415.836425 | -415.713279		3.351	-0.152 | +0.305	3.199 | 3.656	3.364	+0.165
	a′pvqz			-415.912356 | -415.785328		3.457		3.305 | 3.762		+0.059
	a′pv5z			-415.991187 | -415.863015		3.488		3.336 | 3.793		+0.028
	CBS			-416.073854 | -415.944439		3.522		3.370 | 3.827		-0.006
I^- | I	a′pvtz			-294.982288 | -294.865413		3.180	-0.315 | +0.628	2.865 | 3.808	3.059	+0.194
	a′pvqz			-295.061242 | -294.939975		3.300		2.985 | 3.928		+0.074
	a′pv5z			-295.116483 | -294.993899		3.336		3.020 | 3.964		+0.038
	CBS			-295.174430 | -295.050402		3.374		3.059 | 4.002		+0.000

∗ Values from http://physics.nist.gov/PhysRefData/Handbook/index.html

† Values from http://webbook.nist.gov

‡ Shift refers to the difference between the predicted and literature Electron Detachment Energy

Table S5: *Vibrational frequencies for the linear $C_{\infty v}$ halogen and halide-acetylene complexes from CCSD(T) calculations. Frequencies in* cm^{-1} *followed by IR intensities in smaller font in* $\mathrm{km\,mol}^{-1}$. *Also provided are zero point energies (zpe) in* $\mathrm{kJ\,mol}^{-1}$, *mode symmetries, and approximate descriptions.*

		$Cl^-\cdots HCCH$				$Cl\cdots HCCH$				$Br^-\cdots HCCH$		$Br\cdots HCCH$		$I^-\cdots HCCH$		$I\cdots HCCH$		Mode Description
		a′pvtz		a′pvqz		a′pvtz		a′pvqz										
ω_1	σ^+	3455	1.3	3463	1.6	3490	1.85	3496	1.8	3457	0.8	3488	2.6	3462	0.2	3489	<0.1	H-bonded C-H Stretch
ω_2	σ^+	3053	934.7	3068	913.6	3394	128.5	3403	130.2	3126	818.8	3392	143.6	3210	648.6	3395	104.8	Terminal C-H Stretch
ω_3	σ^+	1937	162.1	1947	157	1994	1.0	2002	1.0	1949	125.1	1993	1.6	1962	85.4	1994	0.2	C≡C stretch
ω_4	σ^+	151	34.1	150	33.8	51	0.10	53	0.1	119	11.1	49	0.1	94	4.7	39	<0.1	Intermolecular stretch
ω_5	π	911	71.4	914	68.2	754	157.1	752	164.6	886	67.0	757	150.2	851	68.6	752	137.6	H-bonded H-C-C bend
ω_6	π	594	67.2	605	69.2	603	1.4	617	0.8	597	62.2	605	2.4	600	53.6	600	1.6	Terminal H-C-C bend
ω_7	π	146	<0.1	145	<0.1	46	0.2	27	0.2	138	0.6	53	0.4	124	0.8	54	0.8	Intermolecular Bend
zpe		71.2		71.5		70.2		70.3		71.1		70.3		71.0		70.1		

Table S6: *Vibrational frequencies for the linear C_{2v} halogen and halide-acetylene complexes from CCSD(T) calculations. Unless stated otherwise, calculations employ aug-cc-pVTZ basis sets (cc-pVTZ for H, and PP variants for Br and I). Frequencies in* cm^{-1} *followed by IR intensities in smaller font in* $\mathrm{km\,mol}^{-1}$. *Also provided are zero point energies (zpe) in* $\mathrm{kJ\,mol}^{-1}$, *mode symmetries, and approximate descriptions.*

		Cl···HCCH				Br···HCCH		I···HCCH		Mode Description
		a′pvtz		a′pvqz						
ω_1	a_1	3477	0.8	3484	0.8	3483	<0.1	3484	0.1	H-C symmetric stretch
ω_2	a_1	1961	0.1	1965	0.1	1975	20.6	1983	10.2	C≡C stretch
ω_3	a_1	756	87.9	756	87.3	763	114.2	761	118.1	H-C-C-H in plane symmetric bend
ω_4	a_1	304	0.1	316	0.1	114	9.1	87	4.9	Intermolecular stretch
ω_5	a_2	603	0*	616	0*	595	0*	597	0*	H-C-C-H out of plane asymmetric bend
ω_6	b_1	761	76.2	763	75.7	745	80.7	747	77.9	H-C-C-H out of plane symmetric bend
ω_7	b_2	3388	83.0	3396	84.1	3392	105.2	3392	97.1	H-C asymmetric stretch
ω_8	b_2	591	0.9	600	0.9	614	<0.1	609	0.1	H-C-C-H in plane asymmetric bend
ω_9	b_2	184	0.1	192	0.1	112	0.3	99	0.3	Intermolecular bend
zpe		71.9		72.3		70.5		70.3		

∗ Symmetry forbidden

Table S7: *Cartesian coordinates of the geometries of halogen and halide-acetylene complexes optimised at CCSD(T)/a'pvtz, in* Å. *LA = Linear Anion, LN = Linear Neutral, TN = T-shaped Neutral.*

		x	y	z		x	y	z		x	y	z
	Cl	0.00000000	0.00000000	1.68802813	Br	0.00000000	0.00000000	1.02864912	I	0.00000000	0.00000000	0.75905252
	C	0.00000000	0.00000000	-1.66190256	C	0.00000000	0.00000000	-2.51359721	C	0.00000000	0.00000000	-3.09617622
LA	C	0.00000000	0.00000000	-2.87828856	C	0.00000000	0.00000000	-3.72908145	C	0.00000000	0.00000000	-4.31053736
	H	0.00000000	0.00000000	-0.56869500	H	0.00000000	0.00000000	-1.42560600	H	0.00000000	0.00000000	-2.01450014
	H	0.00000000	0.00000000	-3.94212137	H	0.00000000	0.00000000	-4.79286702	H	0.00000000	0.00000000	-5.37427897
	Cl	0.00000000	0.00000000	1.95662404	Br	0.00000000	0.00000000	1.15490019	I	0.00000000	0.00000000	0.82705321
	C	0.00000000	0.00000000	-2.02464764	C	0.00000000	0.00000000	-2.89802224	C	0.00000000	0.00000000	-3.42899862
LN	C	0.00000000	0.00000000	-3.23539589	C	0.00000000	0.00000000	-4.10882579	C	0.00000000	0.00000000	-4.63983156
	H	0.00000000	0.00000000	-0.95914422	H	0.00000000	0.00000000	-1.83228943	H	0.00000000	0.00000000	-2.36314362
	H	0.00000000	0.00000000	-4.30007781	H	0.00000000	0.00000000	-5.17351480	H	0.00000000	0.00000000	-5.70451627
	Cl	0.00000000	0.00000000	-1.13932452	Br	0.00000000	0.00000000	-0.70812215	I	0.00000000	0.00000000	-0.54252101
	C	0.00000000	0.60781739	1.53053199	C	0.00000000	0.60718160	2.14726102	C	0.00000000	0.60643602	2.64585506
TN	C	0.00000000	-0.60781739	1.53053199	C	0.00000000	-0.60718160	2.14726102	C	0.00000000	-0.60643602	2.64585506
	H	0.00000000	1.67370662	1.54198561	H	0.00000000	1.67301127	2.15789325	H	0.00000000	1.67217955	2.65315003
	H	0.00000000	-1.67370662	1.54198561	H	0.00000000	-1.67301127	2.15789325	H	0.00000000	-1.67217955	2.65315003

Table S8: *Cartesian coordinates of the geometries of chlorine and chloride-acetylene complexes optimised at CCSD(T)/a'pvqz, in* Å. *LA = Linear Anion, LN = Linear Neutral, TN = T-shaped Neutral.*

	x	y	z
	0.00000000	0.00000000	1.68791003
	0.00000000	0.00000000	-1.66356539
LA	0.00000000	0.00000000	-2.87629098
	0.00000000	0.00000000	-0.57166936
	0.00000000	0.00000000	-3.93903510
	0.00000000	0.00000000	1.95004467
	0.00000000	0.00000000	-2.01759905
LN	0.00000000	0.00000000	-3.22476466
	0.00000000	0.00000000	-0.95307100
	0.00000000	0.00000000	-4.28837498
	0.00000000	0.00000000	-1.12587223
	0.00000000	0.60633693	1.51237627
TN	0.00000000	-0.60633693	1.51237627
	0.00000000	1.67110584	1.52478344
	0.00000000	-1.67110584	1.52478344

Table S9: *Energies, Intensities, Franck-Condon factors predicted from ezSpectrum 3.0. Notation for transitions,* 4_0^1*, indicates the transition in* ω_4 *from* $v'' = 0$ *to* $v' = 1$ *with modes numbered according to Table S5. The band origins are from Table S2, i.e. the predicted Adiabatic Detachment Energy (ADE)*

Cl···HCCH				Br···HCCH				I···HCCH			
E	Intensity	FCF		*E*	Intensity	FCF		*E*	Intensity	FCF	
4.0434	6.9710e-03	-8.3492e-02	4_0^1	3.7210	3.6994e-03	+6.0823e-02	0_0^0	3.3320	4.3229e-02	+2.0791e-01	0_0^0
4.0497	3.1558e-02	+1.7764e-01	4_0^2	3.7271	2.7345e-02	-1.6536e-01	4_0^1	3.3369	1.7266e-01	-4.1552e-01	4_0^1
4.0561	8.4694e-02	-2.9102e-01	4_0^3	3.7331	8.9954e-02	+2.9992e-01	4_0^2	3.3417	2.7759e-01	+5.2687e-01	4_0^2
4.0611	9.0002e-03	-9.4869e-02	$4_0^2 7_0^2$	3.7392	1.7165e-01	-4.1431e-01	4_0^3	3.3453	7.0336e-03	-8.3867e-02	7_0^2
4.0625	1.4804e-01	-3.8476e-01	4_0^4	3.7402	5.6670e-03	+7.5280e-02	$4_0^1 7_0^2$	3.3466	2.1968e-01	-4.6870e-01	4_0^3
4.0674	2.4153e-02	+1.5541e-01	$4_0^3 7_0^2$	3.7452	2.0664e-01	+4.5457e-01	4_0^4	3.3502	1.4046e-02	+1.1851e-01	$4_0^1 7_0^2$
4.0688	1.7341e-01	+4.1642e-01	4_0^5	3.7463	1.8641e-02	-1.3653e-01	$4_0^2 7_0^2$	3.3515	7.9024e-02	+2.8111e-01	4_0^4
4.0738	4.2220e-02	+2.0547e-01	$4_0^4 7_0^2$	3.7513	1.5817e-01	-3.9771e-01	4_0^5	3.3550	4.5165e-02	-2.1252e-01	$4_0^2 7_0^2$
4.0752	1.3332e-01	-3.6513e-01	4_0^6	3.7523	3.5573e-02	+1.8860e-01	$4_0^3 7_0^2$	3.3564	6.2759e-03	-7.9221e-02	4_0^5
4.0787	6.8884e-03	-8.2996e-02	$4_0^3 7_0^4$	3.7574	7.1754e-02	+2.6787e-01	4_0^6	3.3599	3.5742e-02	+1.8905e-01	$4_0^3 7_0^2$
4.0802	4.9455e-02	-2.2238e-01	$4_0^5 7_0^2$	3.7584	4.2823e-02	-2.0693e-01	$4_0^4 7_0^2$	3.3612	1.6539e-03	-4.0668e-02	4_0^6
4.0816	6.1010e-02	+2.4700e-01	4_0^7	3.7594	2.8974e-03	+5.3828e-02	$4_0^2 7_0^4$	3.3635	4.5707e-03	-6.7607e-02	$4_0^1 7_0^4$
4.0851	1.2040e-02	-1.0973e-01	$4_0^4 7_0^4$	3.7634	1.4703e-02	-1.2125e-01	4_0^7	3.3648	1.2857e-02	-1.1339e-01	$4_0^4 7_0^2$
4.0865	3.8023e-02	-1.9499e-01	$4_0^6 7_0^2$	3.7644	3.2779e-02	+1.8105e-01	$4_0^5 7_0^2$	3.3661	3.6986e-03	+6.0816e-02	4_0^7
4.0879	1.1721e-02	-1.0826e-01	4_0^8	3.7655	7.3721e-03	-8.5861e-02	$4_0^3 7_0^4$	3.3684	7.3485e-03	+8.5723e-02	$4_0^2 7_0^4$
4.0915	1.0578e-02	+1.0285e-01	$4_0^5 7_0^4$	3.7705	1.4870e-02	-1.2194e-01	$4_0^6 7_0^2$	3.3732	5.8154e-03	-7.6259e-02	$4_0^3 7_0^2$
4.0929	1.7399e-02	+1.3190e-01	$4_0^7 7_0^2$	3.7715	8.8746e-03	+9.4205e-02	$4_0^4 7_0^4$	3.5093	2.1290e-03	+4.6141e-02	$4_0^2 5_0^1 6_0^1$

Continued on next page

Table S9 – continued from previous page

Cl···HCCH				Br···HCCH				I···HCCH			
E	Intensity	FCF		E	Intensity	FCF		E	Intensity	FCF	
4.0964	2.1462e-03	-4.6327e-02	$4_0^4 7_0^6$	3.7755	1.3814e-03	+3.7167e-02	4_0^9	3.5889	1.6015e-03	-4.0019e-02	$3_0^1 4_0^2$
4.0978	1.0843e-02	+1.0413e-01	$4_0^6 7_0^4$	3.7766	3.0470e-03	+5.5199e-02	$4_0^7 7_0^2$	3.5938	1.3412e-03	+3.6623e-02	$3_0^1 4_0^3$
4.0993	3.3429e-03	+5.7818e-02	$4_0^8 7_0^2$	3.7776	6.7932e-03	+8.2421e-02	$4_0^5 7_0^4$	3.7578	1.1446e-03	+3.3833e-02	$2_0^1 4_0^1$
4.1007	2.5954e-03	+5.0945e-02	4_0^{10}	3.7816	1.3408e-03	-3.6617e-02	4_0^{10}	3.7626	1.9672e-03	-4.4353e-02	$2_0^1 4_0^2$
4.2372	2.0236e-03	-4.4985e-02	$4_0^5 5_0^1 6_0^1$	3.7836	2.3112e-03	+4.8075e-02	$4_0^6 7_0^4$	3.7675	1.6980e-03	+4.1206e-02	$2_0^1 4_0^3$
4.3033	1.1565e-03	-3.4008e-02	$3_0^1 4_0^3$	3.9863	1.6347e-03	+4.0432e-02	4_0^3				
4.3097	2.0731e-03	+4.5531e-02	$3_0^1 4_0^4$	3.9924	2.0224e-03	-4.4971e-02	4_0^4				
4.3160	2.5026e-03	-5.0026e-02	$3_0^1 4_0^5$	3.9984	1.6027e-03	+4.0034e-02	4_0^5				
4.3224	2.0004e-03	-4.4726e-02	$3_0^1 4_0^6$	4.1537	1.0295e-03	-3.2086e-02	$2_0^1 4_0^2$				
4.4770	1.4048e-03	-3.7480e-02	$2_0^1 4_0^3$	4.1598	2.0631e-03	+4.5421e-02	$2_0^1 4_0^3$				
4.4833	2.5888e-03	+5.0880e-02	$2_0^1 4_0^4$	4.1659	2.6296e-03	-5.1280e-02	$2_0^1 4_0^4$				
4.4897	3.2277e-03	+5.6813e-02	$2_0^1 4_0^5$	4.1719	2.1616e-03	+4.6493e-02	$2_0^1 4_0^5$				
4.4951	1.2151e-03	-3.4859e-02	$1_0^1 4_0^4$	4.1777	1.0923e-03	-3.3050e-02	$1_0^1 4_0^4$				
4.4961	2.6860e-03	-5.1827e-02	$2_0^1 4_0^6$	4.1780	1.0845e-03	-3.2932e-02	$2_0^1 4_0^6$				
4.5015	1.5313e-03	+3.9132e-02	$1_0^1 4_0^5$								
4.5024	1.3801e-03	+3.7150e-02	$2_0^1 4_0^7$								
4.5079	1.2910e-03	+3.5931e-02	$1_0^1 4_0^6$								